Stress–Strain Properties of Linear Aromatic Polyesters in the Nonlinear Viscoelastic Range*

TIE HWEE NG† and H. LEVERNE WILLIAMS, *Department of Chemical Engineering and Applied Chemistry, University of Toronto, Toronto, Ontario, Canada M5S 1A4*

Synopsis

The stress–strain curves for a series of linear aromatic polyesters were curve-fitted to yield constant parameters for the one-dimensional and three-dimensional constitutive equations for nonlinear viscoelastic properties. Using these constants, the stress–strain curves could be reconstituted somewhat better by the one-dimensional equations, but the agreement with the three-dimensional curves was good. The same constants can be used to predict creep and stress-relaxation, the data for which are in a companion paper.

INTRODUCTION

Linear viscoelastic properties of solid polymers have been studied extensively both experimentally and theoretically. In use, polymeric materials may be subjected to deformations beyond the linear viscoelastic region, and this has prompted some theoretical and experimental studies into the nonlinear range. Eyring and Halsey[1-3] developed a set of one-dimensional constitutive equations based on a model composed of two springs and a nonlinear dashpot. Eyring[4] also drew attention to the relationship of the viscosity of the dashpot to the rate of strain.

These concepts were applied by Haward and Thackray[5] to establish empirical constitutive equations for the one-dimensional treatment of the model with the viscosity varying with the rate of strain; a Hookean spring in series with the combination of an Eyring dashpot and a rubber elasticity spring in parallel. Titomanlio and Rizzo[6,7] extended the concepts to a three-dimensional treatment using the equivalent model of a linear spring in parallel with a Maxwell unit. The viscosity of the dashpot was allowed to change with the rate of strain by an Eyring type mechanism, and the effects of free volume changes were included by use of the Doolittle[8] equation. However, their constitutive equations do not seem to have been extended to stress–relaxation or creep. A revised three-dimensional treatment has been devised which uses a different three-dimensional Maxwell equation suggested by Oldroyd,[9] a vari-

*Presented in part at the 28th IUPAC Macromolecular Symposium, Amherst, MA, Jul. 12–16, 1982, the 22nd Canadian High Polymer Forum, Waterloo, ON, Aug. 10–12, 1983, and the Canadian Society for Chemical Engineering, 33rd Conference, Toronto, ON, Oct. 2–5, 1983.

†Present address: Xerox Research Centre of Canada, Mississauga, ON, Canada.

Journal of Applied Polymer Science, Vol. 32, 4883–4896 (1986)

CCC 0021-8995/86/054883-14$04.00

able viscosity function, and the imposition of constraints in the evaluation of the parameters.[10] Three series of linear aromatic polyesters had been synthesized.[11] These formed series of polymers differing in known ways. It was of interest to study their time-dependent mechanical behavior at large deformations, to describe other nonlinear viscoelastic features of a mechanical model whose constant parameters could be evaluated from the stress–strain data, and to correlate these parameters with the structures of the polyesters which had known chain configurations.

In this paper the stress–strain tests are recorded and used to calculate constants for each polyester by curve fitting. The constitutive equations are used to describe the stress–strain process and the calculated curves are compared to the experimental curves. In a companion paper the same constants are used to predict creep and stress–relaxation and the corresponding theoretical curves compared to the experimental curves.

THEORY

The mathematical derivation of the constitutive equations may be found in the complete work.[10] The one-dimensional equations for the model, illustrated by two Hookean springs and an Eyring nonlinear dashpot, are[5]

$$\sigma = \sigma_1 + \sigma_2 \tag{1}$$

$$\frac{d\sigma_1}{dt} + E_1 K \sinh\left(\frac{V_h \sigma_1}{2kT}\right) = E_1 \frac{d\epsilon}{dt} \tag{2}$$

and

$$\sigma_2 = E_2 \epsilon \tag{3}$$

in which σ is the tensile stress, ϵ is the tensile strain, and E_1 and E_2 are the tensile moduli of the springs. The expression

$$K \sinh\left(\frac{V_h \sigma_1}{2kT}\right) \tag{4}$$

is equal to the rate of strain of the dashpot.[12,13] V_h is the Eyring activation volume, k is Boltzmann's constant, T is absolute temperature, and K is a constant.

The three-dimensional constitutive equations for the model of a Maxwell element in parallel with a rubberlike spring are[6,7]

$$\boldsymbol{\sigma} = \boldsymbol{\sigma}_1 + \boldsymbol{\sigma}_2 \tag{5}$$

$$\boldsymbol{\sigma}_1 = \lambda \dot{\boldsymbol{\sigma}}_1 = 2\eta \mathbf{d} \tag{6}$$

$$\boldsymbol{\sigma}_2 = 2G_2 \mathbf{L}_G \tag{7}$$

Stress $\boldsymbol{\sigma}$ and the Lagrangian finite strain $\mathbf{L}_G$ are represented by their respective tensors of second order. λ is the relaxation time given by η/G_1. G_2 and

G_1 are the elastic moduli of the Maxwell spring and the rubber elasticity spring, respectively. η is the viscosity of the dashpot and d is the rate of deformation tensor.

The time derivative of stress $\dot{\boldsymbol{\sigma}}_1$ is

$$\frac{\mathscr{D}\boldsymbol{\sigma}_1}{\mathscr{D}t} + a\{\boldsymbol{\sigma}_1 \cdot \mathsf{d} + \mathsf{d} \cdot \boldsymbol{\sigma}_1\} \tag{8}$$

in which a is a constant and $\mathscr{D}/\mathscr{D}t$ is the corotational or Jaumann derivative.

A variable viscosity is used and is expressed similarly to Titomanlio and Rizzo,[6] who included the Eyring viscosity equation and the Doolittle free volume effect. The equation was changed by including $|\tau_1|$, the magnitude of the deviatoric stress tensor,[14] as follows:

$$\eta\alpha|\tau_1| \exp\left(\frac{40}{1 + R(\boldsymbol{\sigma}_1:\boldsymbol{\delta})} - B|\tau_1|\right) \tag{9}$$

A rest relaxation time of 20 years is used, R and B are constants with the dimensions of Pa^{-1}, and $(\boldsymbol{\sigma}_1:\boldsymbol{\delta})$ is the first invariant of the stress tensor.[15]

Analysis of the one-dimensional model yields an equation for the stress–strain curve as follows:

$$\sigma = E_2\epsilon + \frac{1}{\phi} \ln\left\{\beta + \sqrt{1 + \beta^2} \tanh\left[\frac{\sqrt{1 + \beta^2}}{2}(E_1\phi\epsilon/\beta + C)\right]\right\} \tag{10}$$

where

$$\phi = \frac{1}{\sigma_1^{\infty}} \ln\left(\beta + \sqrt{1 + \beta^2}\right) = \frac{V_h}{2kT} \tag{11}$$

$$\beta = \dot{\epsilon}/K \tag{12}$$

and

$$C = \frac{2}{\sqrt{1 + \beta^2}} \tanh^{-1}\left(\frac{1 - \beta}{\sqrt{1 + \beta^2}}\right) \tag{13}$$

σ_1^{∞} is the stress at an infinitely long time and $\dot{\epsilon}$ is the rate of strain.

A similar approach for the three-dimensional equations yielded the relationship between stress and strain:

$$\sigma - G_2\left[\frac{(1 + \epsilon)^3 - 1}{1 + \epsilon}\right] + \lambda\frac{V}{l_0}\left\{\frac{\partial\sigma}{\partial\epsilon} - \frac{3(G_1 + G_2) + G_2(1 + a)[1/(1 + \epsilon) + 2\epsilon^2 + 4\epsilon - 1] - 2a\sigma}{(1 + \epsilon)}\right\} = 0 \tag{14}$$

where V/l_0 is $\partial\epsilon/\partial t$, σ is the applied stress, and a is a constant.

The first constraint applied in the calculations is that $E_{sec}/3 > G_2$ which guarantees stress–relaxation rather than stress growth with time. (E_{sec} is the secant tensile modulus.) The second is that $G_2 > E_2/3$, where E_2 is as used in eq. (10). This second constraint arises from the relationships:

$$\frac{d\sigma}{d\epsilon} = 2G_2(1 + \epsilon) = E_2 \tag{15}$$

so that a constraint on ϵ of 0.5 is used. The third constraint is that $40 < B/R < 100$ which assures that the ratio B/R is in a realistic range such that the free volume effect and the Eyring effect on the viscosity of the dashpot are equally important.

EXPERIMENTAL

Chemicals and polymerization technique for the linear aromatic polyesters used in this work were described previously.[11]

The chemical structures are indicated by a code of letters following a number. The number indicates the number of methylene groups in the glycol, nG. T, I, and TcoI indicate the terephthalate, isophthalate, and copolymer series respectively. The well-known Dacron would be 2GT.

Film samples of all nGT, as well as 3GI and 4GI, were prepared by a hot pressing technique using a laboratory press at about 10 K above the melting temperature for 3 min, giving a film thickness of about 0.3 mm and a diameter of about 20 cm. The samples were then removed from the hot press and cooled to room temperature. Solution-cast films were obtained for 6GI, 8GI, 10GI, 3GTcoI, 4GTcoI, 6GTcoI, and 10GTcoI by pouring an approximately 10% solution in dichloromethane onto a glass plate floating on mercury and then drying gradually at room temperature for 2 days. The samples were then dried in a vacuum oven at 313 K for 1 day before storing in a desiccator until used.

All samples were cut in the same direction (e.g., in the radial direction of the circular sheet) into standard shaped dumbbell pieces.

The mean effective length (l_e) of the experimental samples was determined using the technique outlined by Titomanlio and Rizzo.[16] Basically, two lines 3 cm apart were marked at the central portion of the specimen. The samples were elongated in an Instron tensile testing machine at a crosshead speed of 0.5 cm min^{-1}. The machine crosshead was stopped when the yield point was reached. The ratios of the displacements between the two lines and the two jaws of the testing machine were determined and a mean value of the ratio was calculated. The number three divided by the ratio gave the mean effective length of the sample in cm. Subsequently, all strains ϵ were determined using the expression $\epsilon = \Delta l/l_e$, where l_e was found to be 4.5 ± 0.3 cm and Δl is the displacement of the Instron jaws.

The experimental results of load vs. elongation were converted into true stress vs. strain, where the true stress is equal to $(1 + \epsilon)$ times the engineering stress. This is achieved by assuming a constant density.

The tensile elongation tests were performed at room temperature (295 K) by means of an Instron Universal Testing Instrument, floor model TT. Two different elongation rates, 0.5 and 2.0 cm min^{-1}, were chosen. During elonga-

tion, samples were inspected visually to ensure that the deformation was homogeneous throughout the constant cross-sectional region of the test piece. The sample was strained until fracture or until the first sign of necking. The stress–strain curves of the samples cut from the same sheet of film showed very good reproducibility with less than 4% standard deviation. Specimens of the same material prepared from two different sheets of film showed a slightly higher standard deviation of approximately 7%.

RESULTS AND DISCUSSION

To determine the value of a, eqs. (6) and (8) were applied to predict in a steady shear flow the apparent viscosity (η_a) and the first and second normal-stress coefficients (ψ_1, ψ_2), respectively.[15,19]

Table I compares the material functions for some empirical differential models in a steady simple shear flow. The Dewitt model[17] with $a = 0$ predicts a shear-rate dependent apparent viscosity as well as normal stress effects. However, application of this model to the deformation behavior of a solid polymer without rotational motion ($a = 0$) proved to be of little use. The White–Metzner model,[18] with $a = -1$, gives a shear-rate-independent apparent viscosity and zero second-normal stress difference. Although its predictions are not very realistic, it proves to be more useful for engineering calculations where a simple model is needed. With $a = 1$, the first- and second-normal stress coefficients are equal in magnitude and opposite in sign. This result disagrees with viscometric measurements on polymeric materials. From the above three cases, we can conclude that, if the value of a lies within the interval 0 and -1, a more realistic model can be obtained.

When $a = -0.8$ is considered, the model yields a shear-rate dependent viscosity, a positive first-normal stress difference with a shear-rate dependent coefficient, and a negative second-normal stress difference one-tenth the magnitude of the first one. For some time, it was thought that $\psi_2 = 0$ or that it was always negative. Now, some data[19,20] suggest that the ψ_2 may change from a negative sign to a positive sign at high shear rates. This uncertainty allows one to widen the range for the values of a in which the model can be tested against the experimental results.

The dependences of the three-dimensional parameters, B, R, and G_2, on a with $\lambda_0 = 20$ years based on the stress–strain curve of sample 4GT were

TABLE I
Comparison of the Material Functions for some Empirical Differential Models in a Steady Simple Shear Flow

Name of model	Value of a	η_a (Pa s)	ψ_1 (Pa s^2)	ψ_2 (Pa s^2)	$-\psi_2/\psi_1$
Dewitt	0	$\dfrac{\eta}{1+\lambda^2\dot{\gamma}^2}$	$\dfrac{2\eta\lambda}{1+\lambda^2\dot{\gamma}^2}$	$-\dfrac{\eta\lambda}{1+\lambda^2\dot{\gamma}^2}$	0.5
White–Metzner	-1	η	$2\eta\lambda$	0	0
$a = 1$	1	η	$2\eta\lambda$	$-2\eta\lambda$	1
$a = -0.8$	-0.8	$\dfrac{\eta}{1+0.36\lambda^2\dot{\gamma}^2}$	$\dfrac{2\eta\lambda}{1+0.36\lambda^2\dot{\gamma}^2}$	$-\dfrac{0.2\eta\lambda}{1+0.36\lambda^2\dot{\gamma}^2}$	0.1

plotted. The results demonstrated that the three parameters remained essentially constant over the range of a between -1 and 1 except at $a = 0$ where the deviation from the average values seems to be the most. The average values of G_2, R, and B excluding those at $a = 0$ are respectively 71.5 MPa, 6.76 GPa^{-1}, and 0.27 MPa^{-1} for 4GT.

MECHANICAL PROPERTIES

The stress–strain curves of fifteen linear aromatic polyesters are shown in Figure 1. Samples 3GT, 3GI, and 5GT failed by brittle rupture at less than 5% strain due to their relatively high glass transition temperatures,[11] below which the backbone configurations are essentially immobilized. The other samples were stretched to a point where necking or some sign of nonuniform deformation could be visually observed. All curves show similar features; a short linear Hookean range followed by a monotonically increasing range without a sharp yield point or an elastic limit. The curve for 10GI shows a monotonically decreasing range after the yield point followed by a monotonically increasing range. This curve resembles that of a branched polyethylene. One general trend is that the copolyester series and those with longer methylene sequence lengths could sustain large deformations without failure.

Figure 2 shows the dependence of the Young's modulus on the number of (CH_2) groups n in the repeating unit of the three polyester series. The modulus decreases with increasing number of (CH_2) groups and differs from

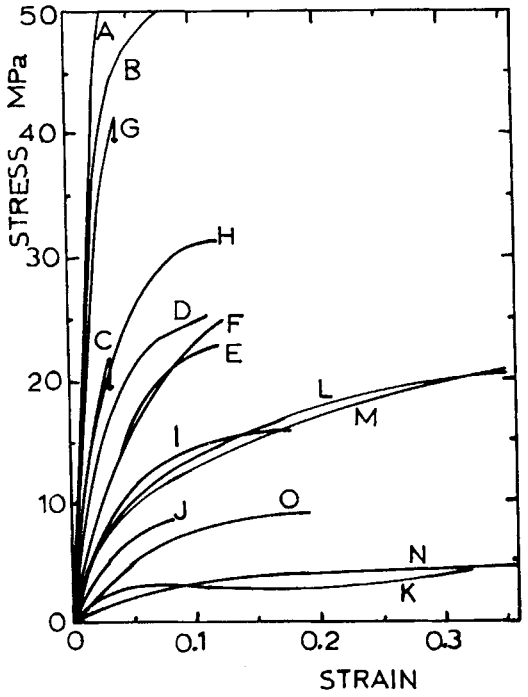

Fig. 1. Stress–strain behavior of aromatic polyesters at 295 K at an elongation rate of 0.5 cm min^{-1}: (A) 3GT; (B) 4GT; (C) 5GT; (D) 6GT; (E) 8GT; (F) 10GT; (G) 3GI; (H) 4GI; (I) 6GI; (J) 8GI; (K) 10GI; (L) 3GTcoI; (M) 4GTcoI; (N) 6GTcoI; and (O) 10GTcoI.

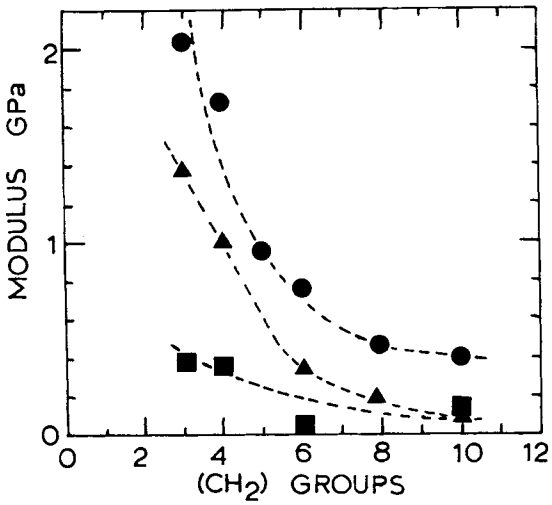

Fig. 2. Young's modulus vs. number of methylene groups in the repeating unit for: (●) terephthalate series; (▲) isophthalate series; (■) copolyester series; (- - -) trend.

one series to the other with the terephthalate series in the highest range. It is interesting to note that the Young's moduli appear to converge to the same value, 0.2 GPa, as the quantity n increases from 3 to 10. With longer methylene sequence lengths, the influence of the phenylene group is outweighted, and the aromatic polyesters behave somewhat like a low density polyethylene the Young's modulus of which is also 0.2 GPa. The three curves could not be combined simply, i.e., normalized.

Table II lists the parameters that were determined for both equations. The values of $a = -0.8$ was used throughout the evaluation of the three-dimensional parameters unless otherwise stated. The quantities G_2 for the terephthalate and the isophthalate series vary with n in the same trend, with the latter in a lower range. The copolyester series shows that G_2 decreases linearly with n, followed by a sharp turn at $n = 6$, reaching the highest value at $n = 0$.

The parameter R, is analogous to the expansibility or compressibility of a material under an external stress. A higher value of R reflects a bigger change in free volume for a given pressure. A general observation is that R increases with n for all three types of polyesters. Longer n-methylene group sequences in the repeating units of the linear chain in the polymer structure result in weaker intermolecular forces. Moreover, Yip and Williams[21] have shown that the crystallinity of these polyesters decreases with increasing number of (CH_2) groups. The crystalline structure in the polymers acts as a filler which could lower the overall expansibility or compressibility of the free volume of the materials.

In the one-dimensional system, the viscosity of the dashpot is related to the Eyring activation volume V_h. It represents the volume of a polymer segment which has to move as a whole for a flow to take place. For the terephthalate and the isophthalate series, V_h increases almost exponentially with the number of (CH_2) groups. However, there is no consistent trend for the copolyester

TABLE II
Parameters used to Predict the Viscoelastic Behavior of Polyester Samples, $\dot{\epsilon} = 6.67^{-1}$

	One-dimensional					Three-dimensional			
Polyester[a]	E_1 (MPa)	E_2 (MPa)	K (s^{-1})	β	V_h(Å^3)	B (10^{-1}MPa^{-1})	R (10^{-2}MPa^{-1})	G_1 (MPa)	G_2 (MPa)
4GT	1600	79.5	1.0×10^{-4}	18.70	6.5×10^2	2.72	0.7	472	70
6GT	700	56.8	5.7×10^{-4}	3.28	8.0×10^2	7.97	1.7	185	58
8GT	425	42.7	4.7×10^{-4}	3.92	9.5×10^2	11.59	2.5	80	60
10GT	320	83.3	3.2×10^{-4}	5.89	1.3×10^3	13.28	3.0	111	15
4GI	940	56.0	1.5×10^{-3}	1.25	2.3×10^2	4.23[b]	1.1	232	30
6GI	320	8.7	5.6×10^{-4}	3.33	1.0×10^3	11.17	2.6	74	21
8GI	140	47.8	3.5×10^{-5}	52.36	7.2×10^3	21.56[b]	5.0	35	28
10GI	98	2.0	5.2×10^{-6}	360.00	2.3×10^4	54.72	12.0	32	14
3GTcoI	350	24.2	8.4×10^{-3}	0.22	1.2×10^2	8.39	2.0	93	7
4GTcoI	340	21.2	2.6×10^{-4}	7.03	1.3×10^2	6.46	1.6	116	4
6GTcoI	38	4.0	4.2×10^{-4}	4.40	5.2×10^3	31.45	7.5	10	1
10GTcoI	114	13.0	41.7×10^{-3}	4.44	2.7×10^3	24.06	7.0	29	13

[a] For significance of codes, see Experimental.
[b] Rest relaxation time = 1 year.

series. The values of V_h obtained here are of the same order of magnitude as those for many different polymers based on the data of Haward and Thackray.[5] The physical significance of V_h may lie in the possible association of the statistical segment volume with it. However, the size of the "statistical link" in the polymer chain is estimated in solution whereas the Eyring volume is observed in the solid polymer. In the solid polymer each chain is surrounded by other polymer chains, so that more than one such link will have to move during a readjustment of relative positions and one would expect V_h to be greater than the size of a statistical link. There are no data available on the volume of the statistical link for comparison with the values reported here for the linear aromatic polyesters studied.

The Young's modulus $3(G_1 + G_2)$, G_2, R, and B as a function of the number of (CH_2) groups, n, for the terephthalate series are in Table II. When fitted by minimization of least-square errors, they conform to the empirical expressions as follows:

$$3(G_1 + G_2) = 11.74n^{-1.52} \quad \text{(GPa)} \tag{16}$$

$$G_2 = 5.34 \times 10^2 n^{-1.31} \quad \text{(MPa)} \tag{17}$$

$$R = 6.74 \times 10^{-10} n^{1.76} \quad (\text{Pa}^{-1}) \tag{18}$$

$$B = 2.8 \times 10^{-8} n^{-1.75} \quad (\text{Pa}^{-1}) \tag{19}$$

These four expressions will be used to predict the creep and stress–relaxation behavior of some new and published data in a companion paper.

COMPARISON OF PREDICTIONS WITH EXPERIMENTAL STRESS–STRAIN DATA

In Figures 3–7, the stress–strain data for the various linear aromatic polyesters, which were replotted from the composite set of curves in Figure 1, have been fitted using the one-dimensional equations (10)–(12) to obtain β, V_h and K, respectively, and the three-dimensional equation (14) by means of the direct search computer program,[22] which yielded the model parameters as given in Table II.

The predictions of the one-dimensional equations are in excellent agreement with all the experimental stress-strain data (Figs. 3–7) except those of 3GTcoI (Fig. 7). In this particular case the best fitting could only be obtained with $\beta = 0.22$, with which the calculated curve could reach the highest possible value of the stress near the yield point region.

The three-dimensional equation prediction is found to be fair. Near the region of the yield points, it gives higher stresses than the experimental results. This is especially distinct in the case of 6GI (see Fig. 6) which does not have a distinct yield point. In Figure 6 the stress–strain data of 10GI have been fitted by omitting the yield behavior. The agreement between the prediction and the experimental curve is regarded as poor.

In Figure 3 samples of 6GTcoI were subjected to two different strain rates, 6.67 and 26.7 h^{-1}. The results show that there is no difference in the elastic

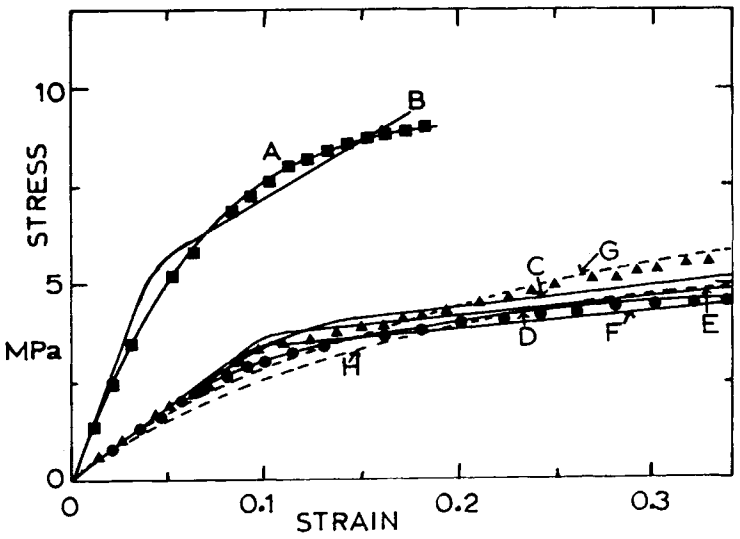

Fig. 3. True stress vs. strain for (■) 10GTcoI, (●) 6GTcoI at 6.67 h^{-1} rate of strain and (▲) 6GTcoI at 26.7 h^{-1} rate of strain: (A) calculated by one-dimensional equations; (B) calculated by three-dimensional equations; (C) one-dimensional at higher strain rate; (D) one-dimensional at lower strain rate; (E) three-dimensional at higher strain rate: (F), three-dimensional at lower strain rate; (G) calculated from linear model equation (20) for the higher strain rate; (H) calculated from linear model equation (20) for the lower strain rate. Parameters taken from Table II. All measurements at 295K.

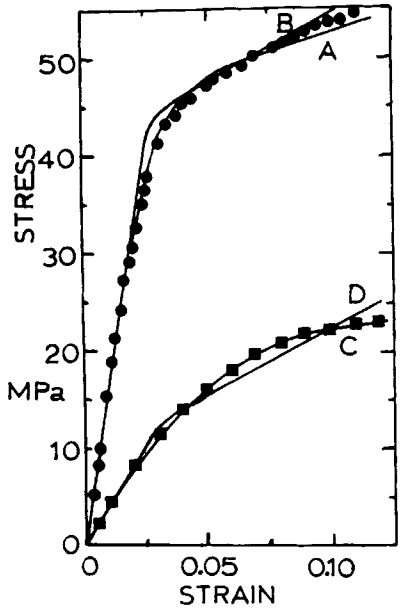

Fig. 4. True stress vs. strain for 4GT (●) and 8 GT (■) at 308 and 295 K, respectively: (A, C) calculated from one-dimensional equations and (B, D) calculated from three-dimensional equations using the parameters in Table II.

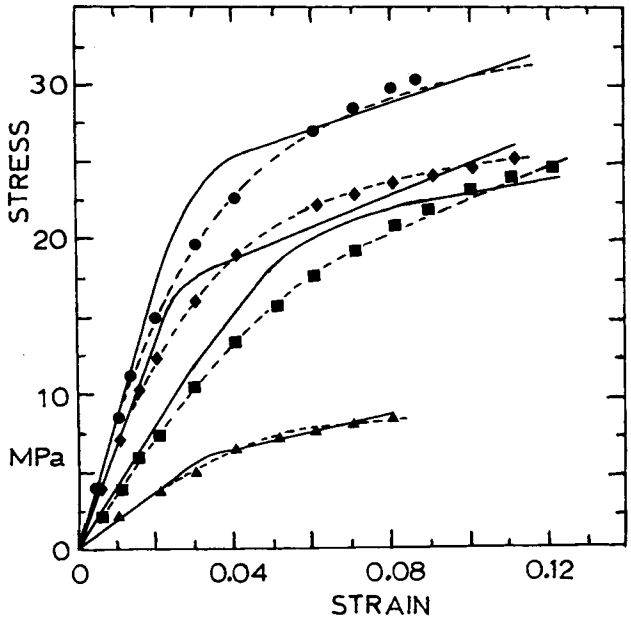

Fig. 5. True stress vs. strain for (●) 4GI, (◆) 6GT, (■) 10GT and (▲) 8GI at 295 K: (- - -) calculated from the one-dimensional equations and (———) calculated from the three-dimensional equations; parameters from Table II.

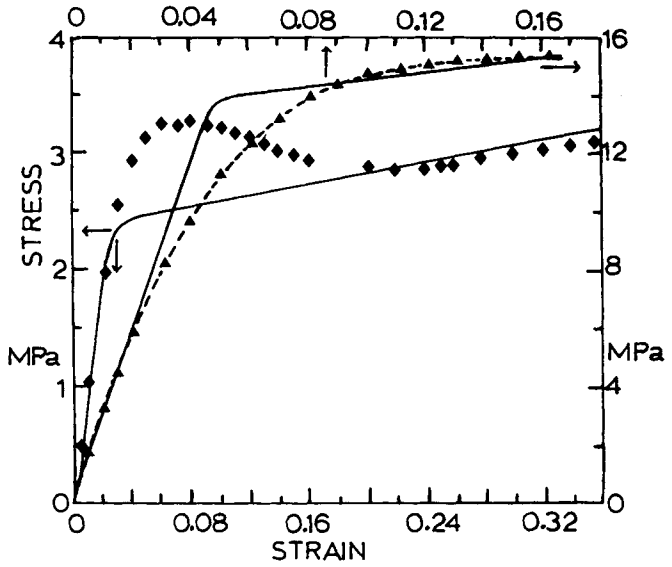

Fig. 6. True stress vs. strain for (▲) 6GI and (◆) 10GI at 295 K: (- - -) calculated from one-dimensional equations; (———) calculated from three-dimensional equations; parameters from Table II.

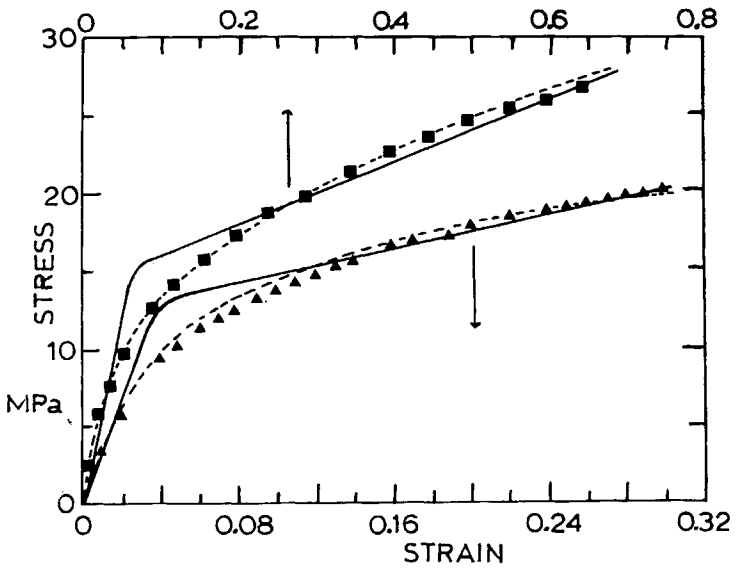

Fig. 7. True stress vs. strain for (▲) 3GTcoI and (■) 4GTcoI at 295 K: (- - -) calculated from one-dimensional equations; (———) calculated from three-dimensional equations; parameters in Table II.

Hookean region of the stress–strain curve. Beyond the linear elastic limit, the stress–strain behavior becomes strain-rate-dependent. The curve with the higher strain-rate is displaced to a slightly higher stress level with a more pronounced yield point. A crosshead speed greater than 2 cm min^{-1} was not used because the samples were seen to develop nonuniform deformation at a very early stage, $\epsilon = 0.13$. The stress–strain equation (14) based on the three-dimensional approach contains the term V/l_0, which makes the predictions for the stress–strain curve dependent on the deformation rate. This is demonstrated in Figure 3. However, the model only predicted a small shift in the stress–strain curve with a fourfold increase in the rate of strain.

The values of G_1 and G_2 do not change with the strain rate. The other two parameters, R and B, change correspondingly with an increase in the strain rate. Their new values at $\dot{\epsilon} = 2.67$ h^{-1} are 0.82 GPa^{-1} and 3.28 MPa^{-1}, respectively, giving a lower viscosity of the dashpot at a higher rate of strain. In Fig. 3, the one-dimensional predictions of the stress–strain data on 6GTcoI at both strain rates are also shown. Similar to the three-dimensional approach, the values of E_1 and E_2 remain unchanged with strain rate while the values of β, K, and V_h change to 14.2, 5.2×10^{-4} s^{-1} and 8000 Å^3, respectively. Also shown in Figure 3 is the theoretical prediction of the stress–strain behavior of 6GTcoI based on a linear model.[23] The model[23,24] is for a typical standard linear solid for which the equation that depicts a stress–strain behavior at a constant strain rate is

$$\sigma = E_2\epsilon + \dot{\epsilon}\eta[1 - e^{-(\epsilon E_1/\eta\dot{\epsilon})}] \tag{20}$$

By fitting the curves of 6GTcoI in Figure 3, the parameters of eq. (20) were found to be $E_2 = 4.6$ MPa and $E_3 = 31.4$ MPa at both strain rates, while

η = 2000 MPa s at $\dot{\epsilon} = 1.85 \times 10^{-3}$ s^{-1} and η = 660 MPa s at $\dot{\epsilon} = 7.41 \times 10^{-3}$ s^{-1}. The viscosity is related to the strain rate by a linear equation, $\eta = 2.45 \times 10^{-3} - 2.41 \times 10^{5}\dot{\epsilon}$, where $\dot{\epsilon}$ is in s^{-1} and η is in MPa s. By substituting the expression for η into equation (20), a single equation is obtained to represent the stress–strain behavior of 6GTcoI at two different strain rates as shown in Figure 3. To obtain a single equation representative of all stress–strain data at all rates would require the incorporation of more Maxwell units to give a spectrum of relaxation times. To avoid complexity, no attempt was made to include more discrete relaxation times in the model.

SUMMARY

Equations developed to enable the prediction of viscoelastic properties from parameters calculated from stress–strain curves were used to calculate or reconstitute the stress–strain curves. The simple one-dimensional equations, based on a one-dimensional model, yielded a better fit than did those based on the three-dimensional interpretation of the same model.

Having to solve for three parameters from the nonlinear constitutive equations simultaneously from a set of stress–strain data subject to several constraints, the direct search computer optimization procedure proved to be very desirable.

Young's modulus decreased with an increasing number of (CH_2) groups in the repeating unit and differed from one series to the other with the terephthalate series highest, the isophthalate series next, and the copolyesters lowest.

Supported by the Natural Sciences and Engineering Research Council of Canada.

References

1. H. Eyring and G. Halsey, *Text. Res. J.*, **16**, 6 (1946).
2. H. Eyring, *Rayon Tex. Mon.*, **71**, 519 (1945).
3. H. Eyring and G. Halsey, *High Polymer Physics*, H. A. Robinson, Ed., Chemical Publishing, New York, 1948.
4. H. Eyring, *J. Chem. Phys.*, **4**, 283 (1936).
5. R. N. Haward and G. Thackray, *Proc. Roy. Soc. London*, *A*, **302**, 453 (1968).
6. G. Titomanlio and G. Rizzo, *Proc. 7th Int. Congr. Rheol., Gothenburg, Sweden, Aug. 23–27*, 522 (1976).
7. G. Titomanlio and G. Rizzo, *Polym. Eng. Sci.*, **18**, 767 (1978).
8. A. K. Doolittle, *J. Appl. Phys.*, **22**, 1471 (1951).
9. J. G. Oldroyd, *Proc. Roy. Soc. London*, *A*, **245**, 278 (1958).
10. T. H. Ng, dissertation, University of Toronto, 1983; *NLC Diss. Abstr. Int. B*, **45** (2), 640 (1984); *Chem. Abstr.*, **101**, 152657m (1984).
11. T. H. Ng and H. Leverne Williams, *Makromol. Chem.*, **182**, 3323, 3331 (1981).
12. G. V. Vinogradov and A. Ya. Malkin, *Rheology of Polymers*, Mir, Moscow, 1980, p. 130.
13. A. S. Krauz and H. Eyring, *Deformation Kinetics*, Wiley-Interscience, New York, 1975, p. 38.
14. S. L. Rosen, *Fundamental Principles of Polymer Materials for Practising Engineers*, Barnes and Noble, New York, 1971, p. 198.
15. G. Astarita and G. Marrucci, *Principles of Non-Newtonian Fluid Mechanics*, McGraw-Hill, London, 1974, pp. 18, 216.
16. G. Titomanlio and G. Rizzo, *J. Appl. Polym. Sci.*, **21**, 2933 (1977).
17. T. W. Dewitt, *J. Appl. Phys.*, **26**, 889 (1955).
18. J. L. White and A. B. Metzner, *J. Appl. Polym. Sci.*, **7**, 1867 (1963).

19. R. B. Bird, R. C. Armstrong, and O. Hassager, *Dynamics of Polymer Liquids*, Wiley, New York, 1977, Vol. 1, p. 147.
20. W. G. Pritchard, *Phil. Trans. Roy. Soc., London, A*, **270**, 507 (1971).
21. H. K. Yip and H. Leverne Williams, *J. Appl. Polym. Sci.*, **20**, 1209 (1976).
22. R. Luus and T. H. I. Jaakola, *AIChE J.*, **19**, 760 (1973).
23. F. J. Lockett, *Nonlinear Viscoelastic Solids*, Academic, London and New York, 1972.
24. D. Roylance and S. S. Wang, *Polym. Eng. Sci.*, **18**, 1068 (1978).

Received January 31, 1985
Accepted March 4, 1986